Turkish Journal of Electrical Engineering & Computer Sciences

http://journals.tubitak.gov.tr/elektrik/

Research Article

Turk J Elec Eng & Comp Sci
(2018) 26: 1572 – 1586
© TÜBİTAK
doi:10.3906/elk-1706-288

High-power density switched reluctance machine development for high-speed spindle applications

Yusuf YAŞA[1,*], **Yılmaz SÖZER**[2], **Muhammet GARİP**[3]

[1]Department of Electrical Engineering, Faculty of Electrical & Electronics, Yıldız Technical University, İstanbul, Turkey

[2]Department of Electrical & Computer Engineering, College of Engineering, The University of Akron, Akron, Ohio, USA

[3]Department of Mechatronics Engineering, Faculty of Mechanics, Yıldız Technical University, İstanbul, Turkey

Received: 23.06.2017 • **Accepted/Published Online:** 21.01.2018 • **Final Version:** 30.05.2018

Abstract: In this study, a high-speed switched reluctance machine (HS-SRM) with cobalt-iron lamination material is proposed for spindle motors, which are used in computer numerical control machines. Wide torque-speed range, high power density, high efficiency, and low cost are the crucial issues in spindle applications. Three types of electric machine candidates, the permanent magnet synchronous machine (PMSM), induction machine (IM), and switched reluctance machine (SRM), are compared with their outstanding features. The SRM spindle motor will offer a more robust, reliable, compact, and cost-effective solution compared to the IM or PMSM spindle applications. Moreover, advancement on cobalt-iron laminations gives a chance to the SRM for competing with the PMSM and IM in terms of power density and efficiency. In this study, a high-speed SRM is designed, optimized, and analyzed. Its performance metrics are obtained based on torque-speed range and efficiency over a wide speed range. The proposed SRM is compared with existing industrial products in terms of power densities. Then the design is verified via experimental study. The results show that the HS-SRM with cobalt-iron lamination material offers ultimate power density and efficiency in wide operating conditions.

Key words: Computer numerical control machines, high-speed applications, high-speed electric machine, milling machines, spindle motor, switched reluctance machine

1. Introduction

In recent years, high-speed electric machines (HSEMs) have gained attention in several applications. Advancement of motor and driving technologies plays an important role for these reasons. Some high-speed (HS) electric machine applications are turbo-compressors and turbo-molecular pumps/blowers, flywheels, high-speed machining-spindle applications, micro gas turbines, turbo-charging in electric vehicles, balancing machines, medical equipment, and military applications [1–4].

HSEM applications provide high mechanical rigidity [4], integrated and compact design with low mass/volume, long maintenance periodicity, and reduction in wear and total losses by eliminating the mechanical transmission [5]. Despite these advantages, electrical and mechanical losses are increased excessively. Core loss becomes dominant in the losses; stray, excess, and bearing losses cannot be ignored because of the high operating

*Correspondence: yasa@yildiz.edu.tr

frequency. Hence, the cooling of the machine is more difficult and needs special attention. Moreover, as the centrifugal forces rise with the rotational speed, mechanical aspects should be carefully taken into consideration.

A typical spindle machine is shown in Figure 1. In spindle applications, machining operations, including milling, cutting, and grinding, gain several benefits with the integration of direct drive high-speed spindles. The required cutting force decreases with an increased cutting speed, which results in enhanced machining accuracy. The surface finish of the operated material is improved as the generated heat does not have sufficient time to conduct to the workpiece. The decreased burr is another big benefit that comes from high cutting speed.

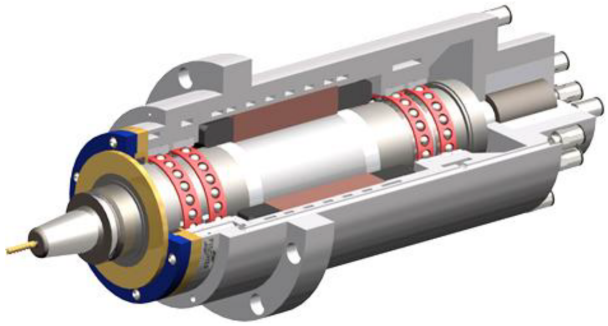


Figure 1. High-speed spindle motor.

In this study, an SRM is developed as a spindle motor. In Section 2, a high-speed concept in electric machines is discussed. HS-SRM performance characteristics are obtained with an optimization in Section 3. In Section 4, the performance of the proposed SRM is compared with the commercially available IMs and PMSMs. The experimental results are given in Section 5. The results are summarized in the conclusion section.

2. High-speed concept in electric machines

The classification for a high-speed electric machine is determined based on the linear velocity of the rotor. The surface centrifugal force on a ring section is calculated as:

$$m = \rho L r \theta \tag{1}$$

$$F_{rad} = mr(2\pi n)^2 \tag{2}$$

$$F_{rad} = 2F_{\tan}\sin(\theta/2) \approx F_{\tan}\theta \tag{3}$$

$$\sigma_t = \frac{F_{\tan}}{Lw} \approx \frac{F_{rad}/\theta}{Lw} = \frac{\rho L r \theta w r (2\pi n)^2}{Lw\theta} = \rho r^2 (2\pi n)^2 = \rho v^2 \tag{4}$$

Here, m is the mass (kg), ρ is the mass density (kg/m^3), L is the axial length (m), r is the mass radius (m), θ is the ring degree ($^\circ$), w is the mass width (m), n is the rotational speed (rpm), v is the velocity (m/s), σ is the mechanical stress (N/mm^2) and F_{rad}, F_{tan} are the radial and lateral forces (N).

The most critical parameter is the centrifugal force on HSEMs as the mechanical stress (σ) is proportional to the mass density and to the square of circumferential speed [6]. For electric machines, the relationship between the rotational and the circumferential speeds is:

$$v = D\pi n \tag{5}$$

Here, D is the rotor outer diameter. In the literature, the threshold value of the circumferential speed for HSEMs is determined as v = 100 m/s. Rotor surface velocities of HSEMs are usually in the range of 100–250 m/s [4].

3. High-speed switched reluctance machine (HS-SRM) design

3.1. HS-SRM design

Motor specifications are determined in Table 1 based on the application requirements. The desired power and the base speed are 1.7 kW and 50 krpm considering natural and liquid cooling options. A high number of poles reduce the torque ripple and acoustic noise. However, the excessive fundamental driving frequency will bring several disadvantages on both the machine and the driver sides. Hence, 6/4 is decided for the pole combination. In this case, the fundamental frequency of the phase current will be 3.3 kHz, which is still considerably higher than conventional electric machines. Special attention is required, such as using Litz wire, thin lamination sheets, etc. [7,8]. In this study, to reduce the iron losses and to increase the power density of the spindle drive, a high-performance HiperCo material is proposed. HiperCo50 contains 48%–50% cobalt element, which provides higher magnetic field saturation level and better mechanical strength. However, its price is excessively higher than that of usual lamination materials, as it is a new technology and it contains cobalt. However, it should be noted that the price of HiperCo50 will be reduced when its usage becomes more widespread. The B-H curves of HiperCo50 and the commonly used M250-35A (M15) materials are compared in Figure 2. When the SRM is operated in the unsaturated region, the torque equation is expressed as in Eq. (6).

Table 1. Design specifications of the developed SRM.

	HiperCo50 laminated SRM	HiperCo50 laminated SRM	Off-the-shelve PMSM (PM4)	Off-the-shelve IM (IM8)	M250-35A laminated SRM
Cooling system [20]	Natural	Liquid	Liquid	Liquid	Natural
Rated power (S1 - 100%)	1.7 kW	3 kW	3.1 kW	2.6 kW	0.98 kW
DC bus voltage	300 V	300 V	300 V	320 V	300 V
Number of phases	3	3	3	3	3
Max. current	15A	25A	15A	15A	10A
Frequency	3.3 kHz	3.3 kHz	1.667 kHz	1.5 kHz	3.3 kHz
Motor rotor pole number	4	4	2	2	4
Motor stator pole number	6	6	-	-	6
Rated rotation speed (krpm)	50	50	50	45	50
Motor type	SRM	SRM	PMSM	IM	SRM
Total weight	3.01 kg	3.06 kg	3.5 kg	4.2 kg	3.01 kg
Frame diameter	90 mm	95 mm	60 mm	80 mm	90 mm
Frame length	120 mm	120 mm	177 mm	181 mm	120 mm

$$T = \frac{\partial W_{ko-alan}}{\partial \theta} = \frac{i^2}{2}\frac{dL(\theta)}{d\theta} \tag{6}$$

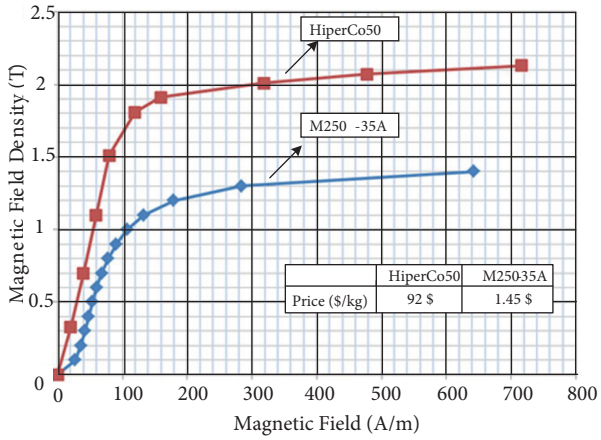


Figure 2. The B-H and price comparison of M250-35A and HiperCo50 lamination materials.

As the slope of each curve in Figure 2 is equal to the inductance, it is clear that cobalt-iron material will enable higher torque and power density than M250-35A silicon-iron lamination material.

The design is processed under finite element analysis (FEA) using ANSYS-Maxwell software. Figure 3 shows efficiency and total loss parameters as a function of air gap length and number of turns for conventional and HiperCo50 laminated HS-SRM. When the air gap length is decreased, the efficiency increases. However, decreasing the number of turns has a negative effect on efficiency as the required phase current rises, which cause iron losses. To reach the same amount of flux linkage in the SRM, HiperCo50 needs less current than conventional lamination. As a result, less phase current reduces the losses. The efficiency curves for conventional and proposed materials are shown in Figure 3. There is no discrepancy in the reduction of air gap length; however, a limitation comes up with the mechanical issue. A 0.4 mm air gap length is selected for the design considering production tolerances.

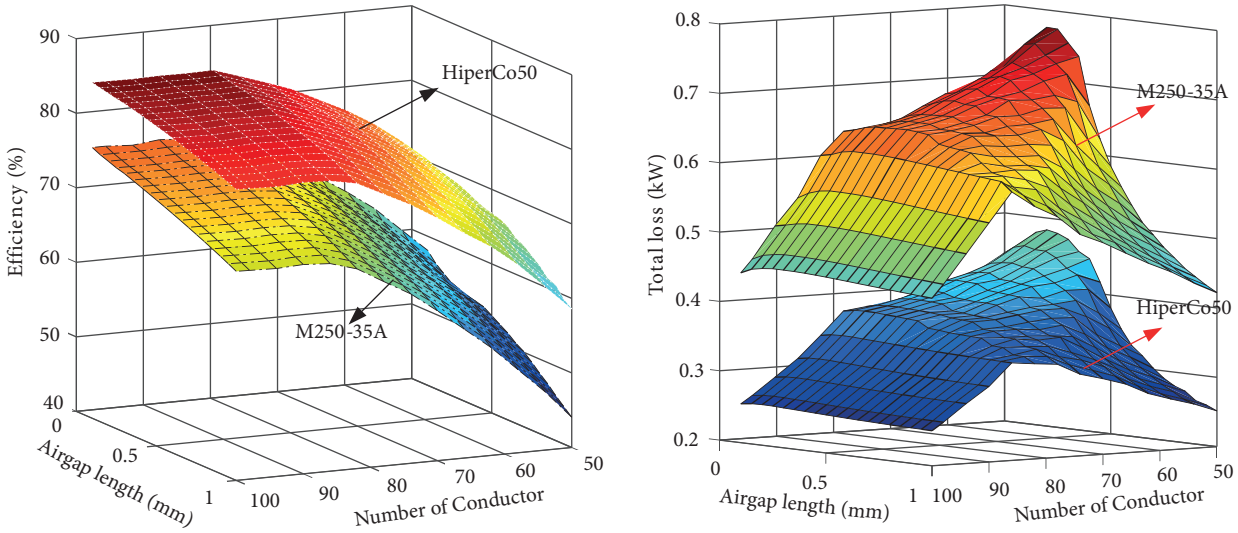


Figure 3. Variation of efficiency and total losses for different air gap lengths and numbers of conductors per slot for HiperCo50 and M250-35A laminated HS-SRM.

Figure 4 presents the performance parameters as a function of stack length and number of turns per pole for a given peak current, which is assumed to be controlled with the hysteresis control method. Increasing both number of turns and stack length provides higher efficiency. However, long stack length causes bulky structure and a high number of turns causes high current density, which causes a high temperature. In totally enclosed natural cooled electric machines, the permissible current density range is 1.5–5 A/mm^2 [9]. This limitation is plotted in Figure 4. A 65 mm stack length and 84 turns are decided based on the aforementioned limitations.

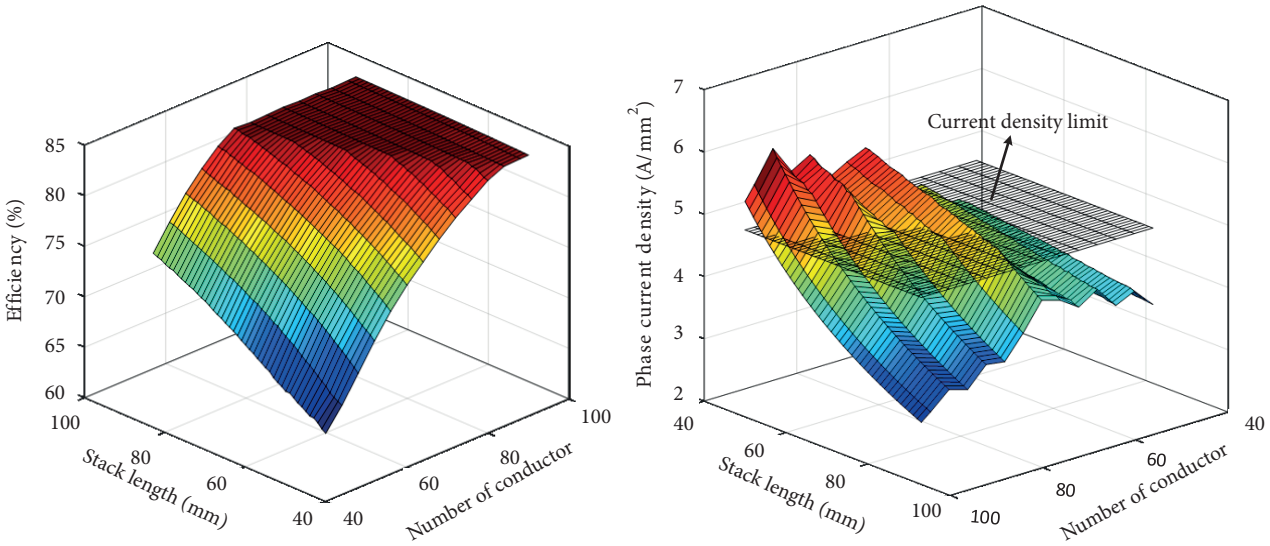


Figure 4. Variation of efficiency and phase current density versus stack length and number of conductors per pole for HiperCo50 HS-SRM.

The stator and rotor pole arc parameters are determined using the study of Lawrenson et al. [10]. The lowest common multiple (LCM) value for pole arcs (B_s, B_r) for 6/4 SRM is:

$$LCM\,(N_s, N_r) = LCM\,(6, 4) = 12 \tag{7}$$

$$min\,(B_s, B_r) > \frac{360}{qN_r} \tag{8}$$

$$min\,(B_s, B_r) > 30^\circ \tag{9}$$

$$B_s + B_r \leq \frac{360}{N_r} \tag{10}$$

Here, $N_s\,N_r$, q are pole number of stator/rotor and number of phases, respectively. Eq. (10) indicates that minimum stator and rotor pole arcs should be at least 30° mechanical degrees. Also, the sum of these two arcs should not exceed 90° for 6/4 SRM. Possible ranges of B_s and B_r pole arcs are drawn in the diagrammatic description shown in Figure 5. More stator pole arc means less winding space and less rotor pole arc means less rotor inertia, which provides fast dynamic response to the SRM with the expense of a high torque ripple. There are four special points on the diagram where the inductance profile has different behavior. Usually the ($1\hat{4}2$) triangle is assumed to be more practical where the rotor pole arc is bigger than the stator pole arc ($B_r > B_s$).

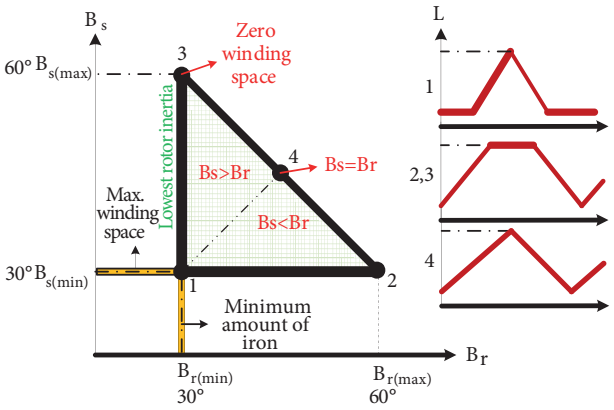


Figure 5. Diagrammatic description of possible pole arcs of stator and rotor.

In computer numerical control (CNC) machines, the dynamic response of the operating spindle plays an important role in the fast operation. Hence, the rotor pole arc should be determined at the lowest value possible in the 6/4 SRM combination. A bigger slot area can be provided by choosing the stator teeth smallest arc value as much as possible. In conventional SRMs, keeping the teeth small causes high magnetic field densities in the lamination, which is considered as a drawback in terms of saturation and efficiency. However, cobalt-iron lamination material can handle high magnetic fields. Thus, the stator pole arc is kept at a minimum value that is 30° mechanical degrees. In the second step, the rotor pole arc is optimized with the efficiency goal.

Two parallel branches are determined in the HS-SRM to minimize the eccentricity effect that might cause failure at high speeds. Moreover, the stator yoke thickness is minimized as much as possible to reduce current density by enabling a big slot area. Rotor yoke thickness should be also minimized for low inertia; however, there will be high mechanical stress. The optimized values and the related design geometry are provided in Table 2 and Figure 6, respectively.

Table 2. Optimized parameters of developed HS SRM.

Stator pole arc	β_s	30°	Stator inner diameter	D_{is}	40 mm
Rotor pole arc	β_r	33.3°	Stator outer diameter	D_{os}	77 mm
Stator yoke thickness	Y_s	5.9 mm	Stack length	L_{stack}	65 mm
Rotor yoke thickness	Y_r	6.1 mm	Number of turns per pole	N_s	84
Shaft diameter	D_{ir}	15 mm	Number of parallel branches	p_s	2
Rotor outer diameter	D_{or}	39.2 mm	Wire diameter	mm	0.643

3.2. HS-SRM performance analysis

First of all, static electromagnetic analysis is executed for the developed SRMs to get static torque and flux data as a function of position and phase current. Then, using the SRM static performance data, SRM control parameters will be determined. The analyses are performed with a coupled simulation method. The control algorithm is developed in MATLAB-Simulink and linked to the ANSYS-Simplorer where the power converter model exists. Then the FEA model of the SRM is linked to the power converter model. There is an additional algorithm that optimizes and determines the reference current level and the turn-on and turn-off angles.

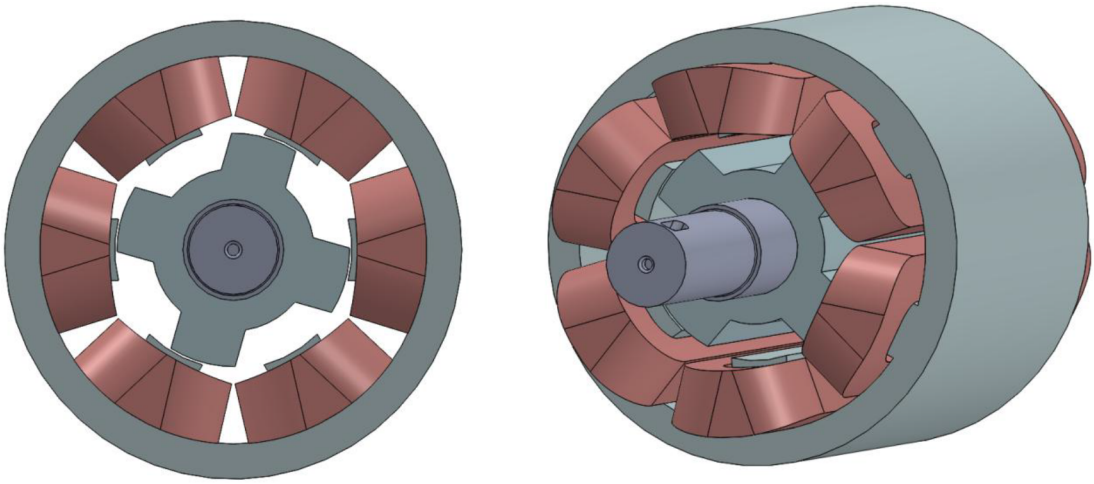


Figure 6. The 2D and 3D geometry of the developed SRM.

3.2.1. Optimization of turn-on and conduction angle

Optimization of turn-on and turn-off angles can be performed under different goals such as minimum torque ripple (MTR), maximum average torque (MT), and maximum average torque per ampere (MTPA). The MTPA is chosen for performance analysis as it is more efficient in SRM driving than the other two methods. The definition of the turn-on and turn-off angles is given in Figure 7. The results are provided in Figure 8. Figure 8a shows the torque per ampere values at different excitation angles at 50 krpm operating speed. The MTPA value is always reached on the single pulse switching boundary as shown in Figure 8a. The right side of the boundary is a hysteresis mode switching area where the phase currents are regulated at the determined reference currents. On the other hand, the left side of the boundary is the single pulse switching area where the phase current does not reach the desired reference value with related switching angles. As the MTPA value is found in the single switching boundary, this case will offer another big advantage on the converter side: semiconductors will be operated at relatively lower frequencies. Thus, the converter efficiency increases, as well. Figures 8b and 8c show the dynamic torque behavior and phase currents, respectively. With a 12 A reference current and 5.65 Arms phase current, the HS-SRM is able to generate 1.7 kW output power with natural cooling.

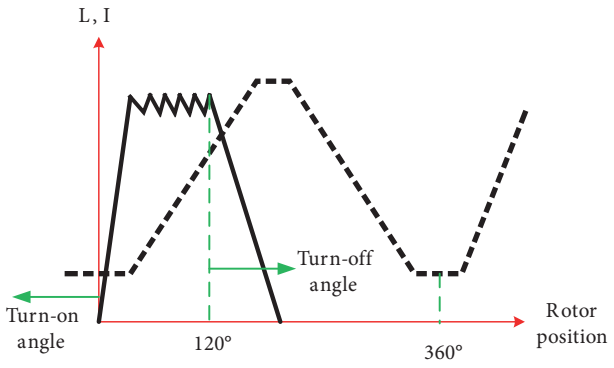


Figure 7. Definition of turn-on and turn-off angle.

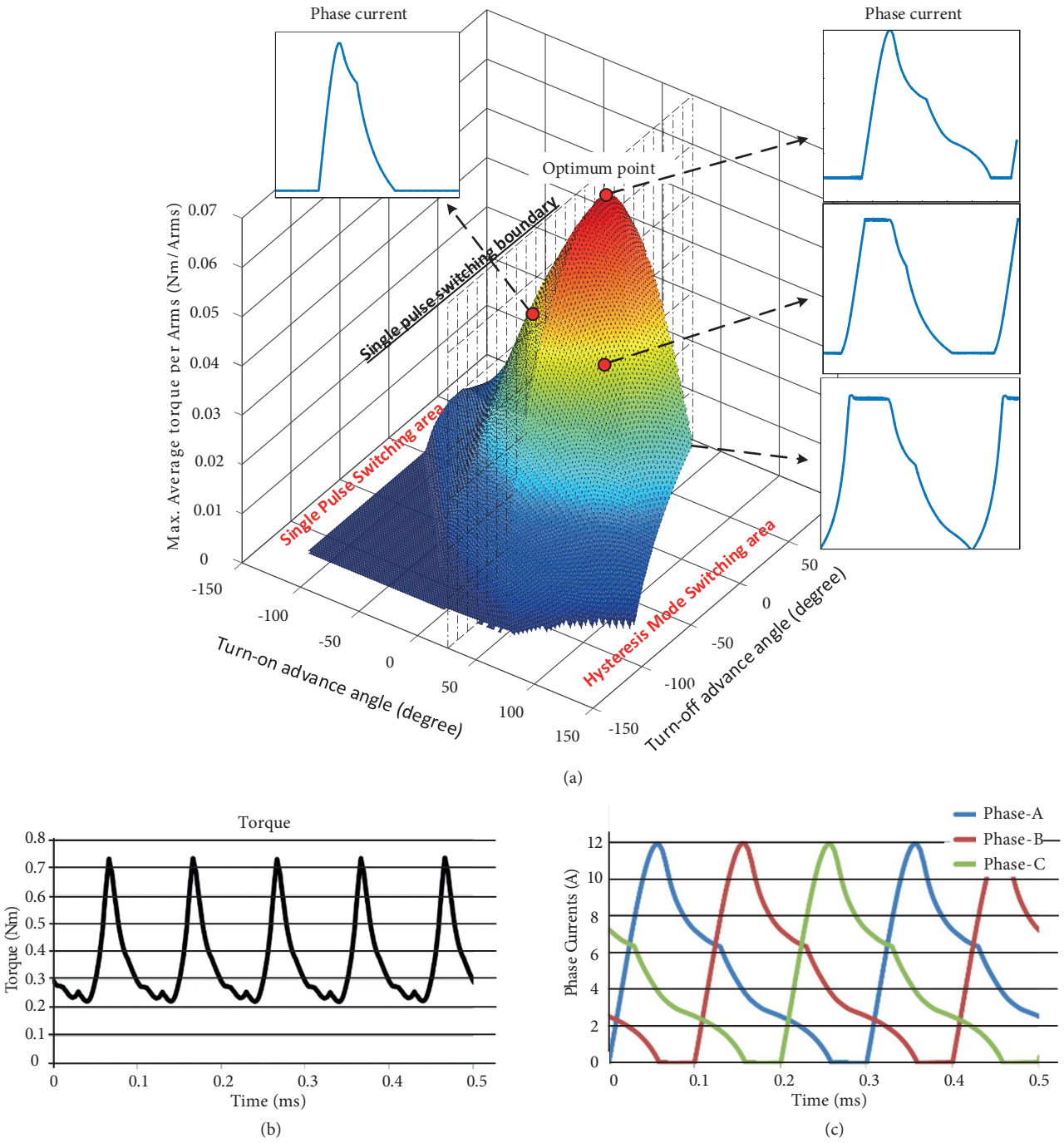


Figure 8. Dynamic MTPA performance of natural cooled HS-SRM on rated condition where I_{ref} = 12 A, θ_{on}= 26°, and θ_{off}= 10° at 50 krpm.

3.2.2. Torque-speed characteristic curve

Wide speed-torque range and high peak torque capability are always desired in spindles.

The combination of the high peak torque and low rotor inertia enables a high acceleration rate. In terms of inertia, as the SRM does not have any winding or magnet in the rotor, it provides better acceleration

rates compared to the PMSM and IM. In terms of peak torque capability, high peak torque is possible by pushing high phase current in the SRM. However, in the PMSM and IMs, the peak current is limited by magnet demagnetization risk and slip, respectively. The torque-speed curve of the SRM is obtained by applying an optimal current waveform at each speed. The curve is provided in Figure 9. Natural cooled and liquid cooled designs are pointed out in the figure. Nominal operating conditions for both cooling options are determined by performing numerical thermal analyses. The results are not shared here to avoid complexity.

3.2.3. Efficiency map

An efficiency map is a contour plot of the efficiency on speed and torque axes [11]. In the analysis, copper losses, core losses, and friction losses are taken into consideration. The core losses are the major part of the losses and the calculation is not straightforward. Thus, coupled simulation FEA is performed to calculate the iron losses.

The bearing friction loss depends on the rotational speed and can be estimated with Eq. (14), where M is the frictional moment, μ is the friction coefficient of the bearing, p is the equivalent dynamic bearing load, d is the bearing bore diameter, and n is the rotor speed. From the efficiency map in Figure 10, the results show that the developed SRM's efficiency is around 70%–80% in a wide speed range.

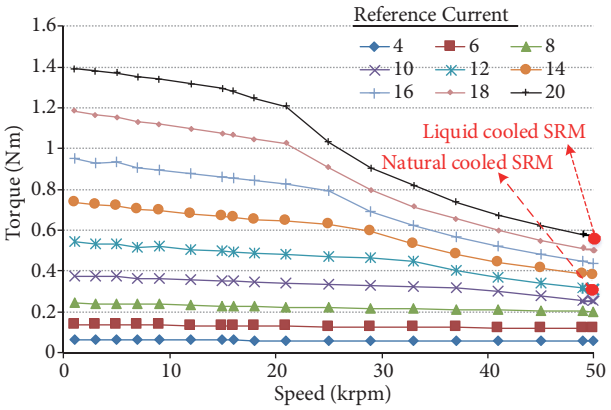


Figure 9. Torque-speed curves of developed SRM for different excitation currents.

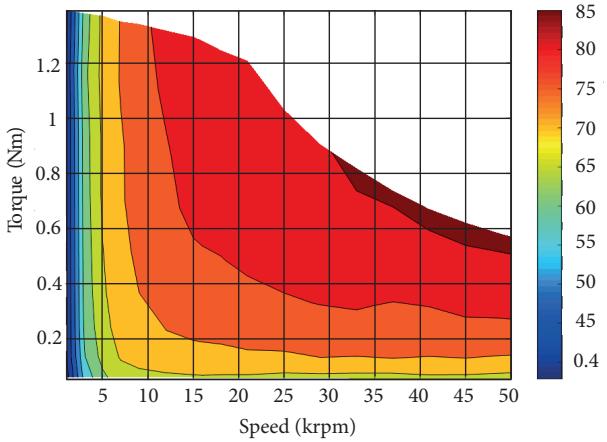


Figure 10. Efficiency map of developed SRM; torque-efficiency curve in a speed range.

$$\eta = \frac{P_{out}}{P_{in}} \tag{11}$$

$$P_{in} = P_{out} + P_{cu} + P_{core} + P_{friction} \tag{12}$$

$$P_{cu} = 3(I_{rms})^2 R_{phase} \tag{13}$$

$$P_{friction} = 1.05Mn10^{-4} = \frac{1.05(10^{-4})}{2}\mu pdn \tag{14}$$

4. Comparison of different spindle motor technologies

Integrated direct-drive spindles became a new trend for new technology CNC machines. The integration eliminates the need for a belt or gear, which are used for mechanical power transmission.

PMSMs and IMs are commonly used in spindles [5,12], whereas switched reluctance machines are not available in the industry [13]. These three types of electric machines are compared with different viewpoints in Table 3 [14–18].

Table 3. Comparison of HS electric machine types.

	PMSM	IM	Conventional SRM	1: Excellent 2: Fair 3: Bad
Power density	1	3	2	
Vibration/noise	1	2	3	
Efficiency	1	3	2	
Rotor temperature	1	3	2	
Price	3	2	1	
$\cos\varphi$	1	2, 3	3, 2	
Reliability	3	2	1	
Availability	2	1	3	
Complexity	3	2	1	
Maximum load ability	1	3	2	
Robustness	3	2	1	

In spindle applications, a wide speed-torque range, high power density, high efficiency, and low cost can be considered as the crucial requirements [14]. The IM is the most famous in spindles because of the price and accessibility in the market. Nevertheless, high performance in the compact design is a new trend. The PMSM is gaining attention, but the magnet cost is a drawback and limits its market penetration. In addition, centrifugal forces cause mechanical stress on the magnets. A protective sleeve with carbon fiber, glass fiber, or titanium alloys is needed to fix the magnets [2]. However, the SRM is known as a reliable, fault-tolerant, simple, and cheap electric machine. As the rotor only contains steel lamination, there is no mechanical stress limit on the rotor [19]. With the use of high-performance core material, SRMs can have competitive efficiency and performance.

The proposed SRM is compared with commercially available IMs and PMs having similar power ratings and cooling methods. The developed SRMs in both cooling methods, a conventional SRM that has the same geometry as the developed SRM but has M250-35A lamination more in the core, and the present industrial products are compared as shown in Figure 11 in terms of their power densities based on weight. It should be noted that the comparison is performed in continuous operation so the output power limiting factor is the thermal behavior (or the power loss) in each electric machine. The results show that the naturally cooled conventional SRM can give 0.98 kW with the HiperCo50 utilized SRM size. However, the HiperCo50 utilized SRM can give 1.71 kW, which shows the effectiveness of the material selection. It should be noted here that it is also possible to use cobalt-iron lamination material in PMSMs, but the big limitation factor will emerge at high magnetic fields as the magnets can go into the irreversible demagnetization area where the magnets are damaged. However, in SRMs, there is no magnet, so the only limiting factor is the lamination material. Reported industrial products have a liquid cooling and the proposed SRM has natural and liquid cooling options. Figure

11 shows that the developed SRM with natural cooling can compete with some industrial products. However, the liquid cooled SRM is superior to any other type of products.

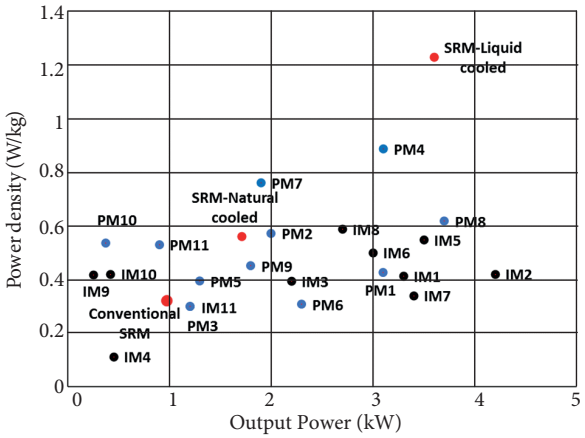


Figure 11. The power density comparison of proposed SRM designs and present industrial products.

5. Experimental study

The designed and analyzed high-speed SRM is produced and tested. The produced SRM is shown in Figure 12. Cobalt-iron (Co-Fe) lamination material is cut with the wire electrical discharge machining (wire-EDM) method and annealed at 1600 °C to achieve high magnetic permeability. The laminated sheets are bonded using glue, then cured at high temperature. Litz wire is used to minimize the phase resistances at higher frequencies. The rotor position sensing is done by using an absolute encoder. Usually, ceramic or hybrid ball bearings are preferred in high-speed applications as they can withstand high temperatures without deformation. However, they are much more expensive than steel ball bearings. As the prototyped SRM will be tested in a short time (not as much as industrial products), premium steel ball bearings with tight production tolerances are utilized. The size of the developed SRM is compared with an off-the-shelf PMSM spindle as shown in Figure 13. As expected, the proposed SRM has a big advantage in terms of size and weight because of the Co-Fe lamination.

The proposed high-speed SRM is coupled to the hysteresis brake, which is behaving as a dynamometer. The phase inductances are measured using an LCR meter for different rotor positions. The simulation and measured inductance profiles are compared in Figure 14a, where the measured data has 15% less slope than what is expected. As the SRM's torque is proportional to the rate of change of inductance, the same amount of reduction is expected in torque. The HS-SRM dynamic performance tests are conducted until 15 krpm as shown in Figure 14b as the test setup is not suitable for higher speeds. The measured electromagnetic torque values at different speeds and currents are given in Table 4. The results verify the inductance deviation between the FEA and experimental data.

6. Conclusion

In this study, HS-SRM with cobalt-iron lamination material is developed for direct drive spindle applications. High-speed applications are briefly mentioned and the benefits are discussed. PMSMs and IMs are broadly utilized in spindle applications. PMSMs provide high power density and IMs provide cost-effective solutions. In this study, SRM with HiperCo50 cobalt-iron lamination material is proposed as an alternative electric machine. It is known that conventional SRMs have a lower power density compared to PMs. By using cobalt-iron

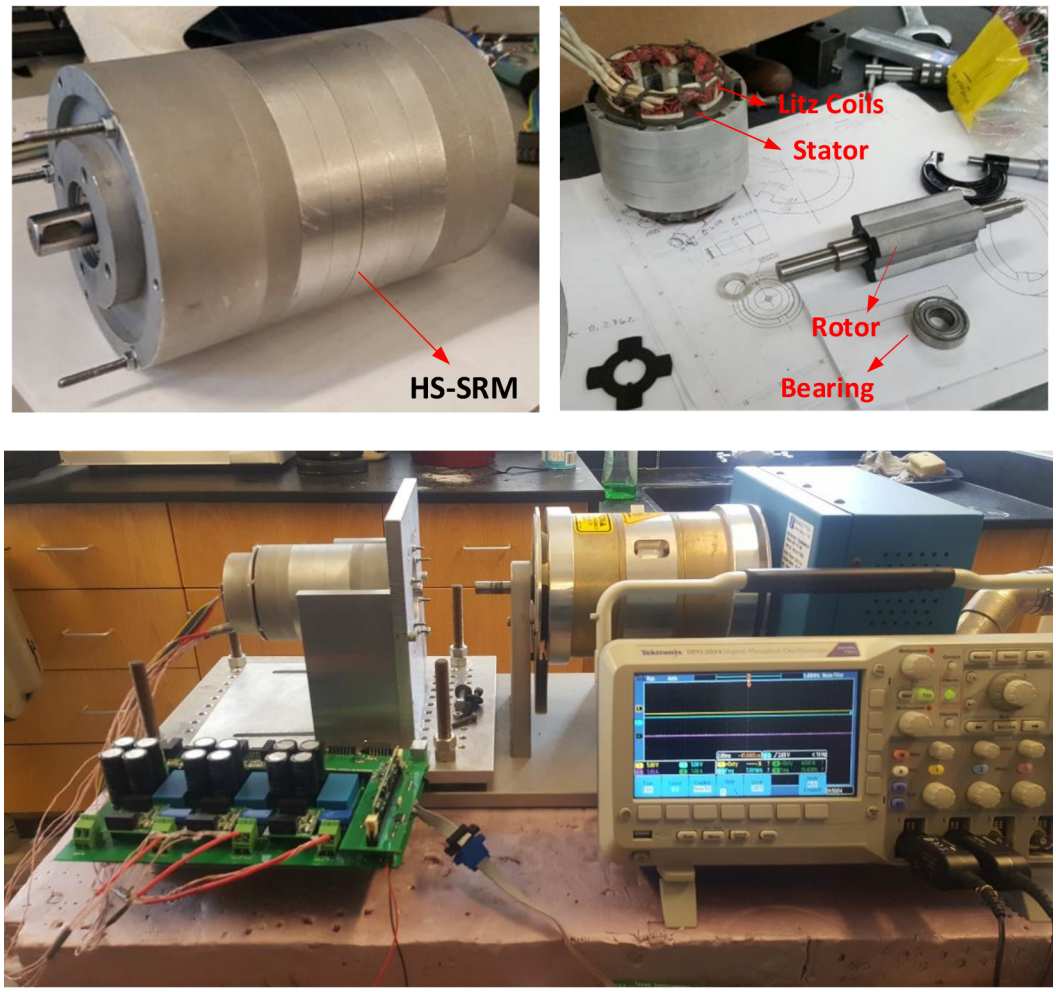


Figure 12. The photo of the produced high-speed SRM and test bench.

Table 4. Experimental test results of the HS-SRM.

Ref. current (A)	DC bus voltage	Mechanical speed (rpm)	FEA torque (Nm)	Experimental torque (Nm)	Measured output power (W)	Deviation (%)
10 A	170	10,000	0.339	0.268	281	20.94
12 A	100	10,000	0.3864	0.341	357	11.75
16 A	150	9000	0.7799	0.672	633	13.84
20 A	170	10,000	1.13	0.96	1005	15.24
16 A	170	15,000	0.7037	0.565	887	19.71

lamination material, the power density is increased without compromising other SRM advantages such as robustness, reliability, compactness, and cost-effectiveness. In addition, due to the absence of any winding or magnet in the rotor, the SRM can provide high torque over a wide speed range and high dynamic response with low inertia/high acceleration rate. These outstanding features will make the SRM suitable for grinding,

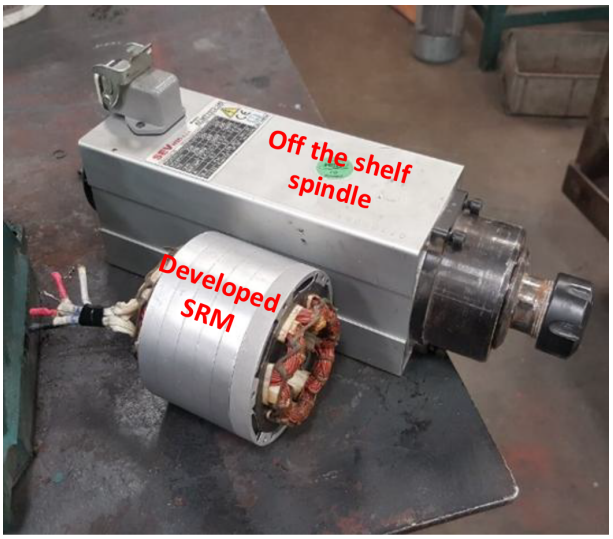
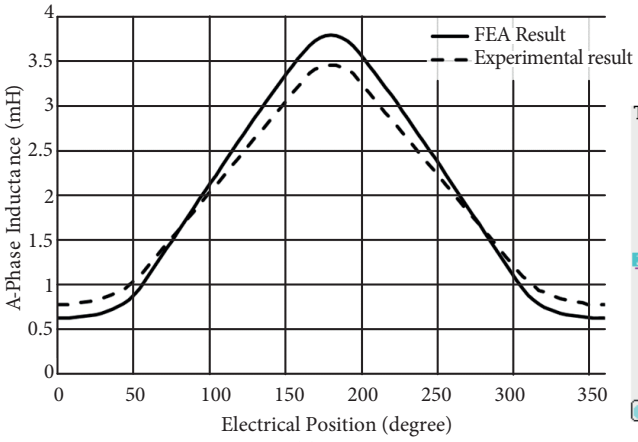
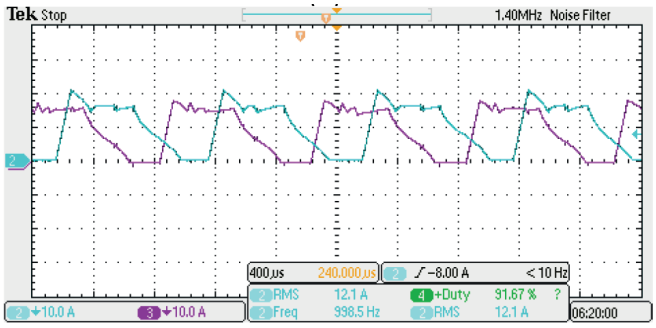


Figure 13. The size comparison of the developed SRM and off the shelf PMSM spindle and wiring of the stator.



(a)



(b)

Figure 14. The comparison of FEA and measured phase inductances and the phase-A and phase-B current waveforms at 15 krpm mechanical speed and 170 V DC bus with 16 A reference phase current.

milling, and cutting spindles. The SRM is designed with the rating of 1.7 kW and 3 kW at 50 krpm for natural and liquid cooling options, respectively. Its performance metrics are obtained based on torque-speed range and efficiency behavior over a wide speed range. The developed SRM is compared with existing industrial products. The results show that the proposed HS-SRM offers high power density and high efficiency in wide operating conditions. Finally, experimental results are provided to verify the design. A limited difference between the simulation and experimental, which is around 15%, is achieved. The results indicate that the SRM with high-quality core material may be an attractive candidate for spindle applications.

7. Acknowledgment

This study was supported by the Scientific and Technological Research Council of Turkey (TÜBİTAK). The Scientific and Technological Research Council of Turkey is acknowledged for granting the first author with support for international doctoral research study in the framework of a TÜBİTAK-BİDEB 2214 grant.

References

[1] Tursini M, Villani M, Fabri G, Di Leonardo L. A switched-reluctance motor for aerospace application: design, analysis and results. Electr Pow Syst Res 2017; 142: 74-83.

[2] Binder A, Schneider T, Klohr M. Fixation of buried and surface mounted magnets in high-speed permanent magnet synchronous motors. In: IEEE 2005 IAS Annual Meeting; 2–6 October 2005; Kowloon, Hong Kong. New York, NY, USA: IEEE. pp. 2843-2848.

[3] Munteanu G, Binder A, Schneider T. Loss measurement of a 40 kW high-speed bearingless PM synchronous motor. In: IEEE Energy Conversion Congress and Exposition; 17–22 September 2011; Phoenix, AZ, USA. New York, NY, USA: IEEE. pp. 722-729.

[4] Binder A, Schneider T. High-speed inverter-fed AC drives. In: IEEE 2007 International Aegean Conference on Electric Machines and Power Electronics; 10–12 September 2007; Ankara, Turkey. New York, NY, USA: IEEE. pp. 9-16.

[5] Tenconi A, Vaschetto S, Vigliani A. Electrical machines for high-speed applications: design considerations and tradeoffs. IEEE T Ind Electron 2014; 61: 3022-3029.

[6] Binder A. High speed drives-tutorial. In: IEEE International Conference on Electrical Machines; 2–5 September 2014; Berlin, Germany. New York, NY, USA: IEEE.

[7] Reddy PB, Jahns TM. Analysis of bundle losses in high speed machines. In: IEEE International Power Electronics Conference; 21–24 June 2010; Sapporo, Japan. New York, NY, USA: IEEE. pp. 2181-2188.

[8] Bartoli M, Noferi N, Reatti A, Kazimierczuk MK. Modeling Litz-wire winding losses in high-frequency power inductors. In: IEEE Annual Power Electronics Specialists Conference; 23–27 June 1996; Baveno, Italy. New York, NY, USA: IEEE. pp. 1690-1696..

[9] Staton D. Enhancements in the electric machine cooling analysis. In: Motor and Drive Systems Conference; 29–30 January 2014; Orlando, FL, USA. pp. 1-34.

[10] Lawrenson PJ, Stephenson JM, Blenkinsop PT, Corda J, Fulton NN. Variable-speed switched reluctance motors. IET Electr Power App 1980; 127: 253-265.

[11] Mahmoudi A, Soong WL, Pellegrino G, Armando E. Efficiency maps of electrical machines. In: IEEE Energy Conversion Congress and Exposition; 20–24 September 2015; Montreal, Canada. New York, NY, USA: IEEE. pp. 2791-2799.

[12] Moghaddam RR. High speed operation of electrical machines, a review on technology, benefits and challenges. In: IEEE Energy Conversion Congress and Exposition; 14–18 September 2014; Pittsburgh, PA, USA. New York, NY, USA: IEEE. pp. 5539-5546.

[13] Laboid C, Srairi K, Mahdad B, Benchouia MT, Benbouzid M. Speed control of 8/6 switched reluctance motor with torque ripple reduction taking into account magnetic saturation effects. In: Elsevier International Conference on Technologies and Materials for Renewable Energy, Environment and Sustainability; 17–21 April 2015; Beirut, Lebanon. Amsterdam, the Netherlands: Elsevier. pp. 112-121.

[14] Hendershot JR. High speed permanent magnet brushless motors for spindles and compressors. In: Incremental Motion Control Systems Society 1996; Hillsboro, OH, USA. pp. 123-146.

[15] MacMinn SR, Jones WD. A very high speed switched-reluctance starter-generator for aircraft engine applications. In: IEEE National Aerospace & Electronics Conference; 22–26 May 1989; Dayton, OH, USA. New York, NY, USA: IEEE. pp. 1758-1764.

[16]] Hofmann H, Sanders SR. High-speed synchronous reluctance machine with minimized rotor losses. IEEE T Ind Appl 2000;36: 531-539.

[17] Soong WL, Kliman GB, Johnson RN, White R, Miller J. Novel high speed induction motor for a commercial centrifugal compressor. In IEEE Industry Applications Conference, 34th IAS Annual Meeting; 3–7 October 1999; Phoenix, AZ, USA. New York, NY, USA: IEEE. pp. 494-501.

[18] Yang Z, Shang F, Brown IP, Krishnamurthy M. Comparative study of interior permanent magnet, induction, and switched reluctance motor drives for EV and HEV applications. IEEE T Transport Electrific 2015; 1: 245-254.

[19] Radun AV. Design considerations for the switched reluctance motor. IEEE T Ind Appl 1995; 31: 1079-1087.

[20] Yasa Y, Sincar E, Ertugrul BT, Mese E. A multidisciplinary design approach for electromagnetic brakes. Electr Pow Syst Res 2016; 141: 165-178.